ESTIMATING THE STABILITY DOMAIN OF SYMPLECTIC MAPS: A ROBUST METHOD VIA A BOUNDING-SET OF UNSTABLE INITIAL CONDITIONS

I. Morozov * †, Elettra-Sincrotrone Trieste S.C.p.A., Trieste, Italy
M. Giovannozzi ‡, CERN, Geneva, Switzerland

Abstract

Estimating the stability domain in view of its characterisation and optimisation is one of the primary topics of single-particle non-linear beam dynamics. The boundary of the stability domain, the dynamic aperture (DA), has a complicated fractal structure that cannot be reliably estimated by analytical means. Instead, numerical methods are used to estimate the DA, with the additional constraint of identifying only the domain that is simply connected around the origin. The most common case of a DA estimate for 4D systems can be reduced to a lower-dimensional angular scan, thus lowering the computational burden. Here we present a new robust method of DA characterisation based on constructing a cloud of escaping initial conditions that bounds the stable domain and has a significantly lower computational complexity than a direct scan of phase-space variables. The proposed method is applied to a non-linear 4D symplectic map, and the results are compared with those obtained using standard methods, both in terms of accuracy and CPU time.

INTRODUCTION

The DA remains one of the main concepts characterising non-linear performance in currently operating and proposed circular charged-particle accelerators such as the CERN LHC [1] and FCC [2, 3]. Relevant effects include the impact of DA on injection efficiency and beam lifetime. Although strict stability would require initial conditions to remain within the DA region indefinitely, in practice, DA is commonly defined as a finite-time simply connected stable region around the origin [4]. Accurate computation of DA requires repeated iterations of the map representing one-turn propagation in the ring. The number of iterations per initial condition can range from the order of 10^3 for electron light sources, corresponding to a characteristic time scale over which synchrotron radiation produces sufficient damping [5], to 10^7 for proton machines, where synchrotron radiation has a negligible effect [6], considering that ultimately the timescale is also dependent on the duration of the process under consideration, e.g. collisions in the LHC, which is of the order of several hours, corresponding to about several 10^8 iterations. As a result, direct DA computation is a computationally demanding task.

The standard approach to DA estimation is based on iterating initial conditions along rays starting from the origin, which is assumed to be an elliptic fixed point [7]. This provides a significant computational gain compared with scanning a full rectangular grid of initial conditions and directly targets the main central stable region. This method assumes that the DA region has a sphere-like shape, or more generally, that it is star-shaped, and computes the DA volume using a structured grid of angular variables in polar coordinates together with the corresponding equivalent hypersphere radius as the main DA characterisation parameter. In addition to ray-based DA computation, modern algorithms [8], as well as machine learning methods [9–13], are actively being developed to reduce the computational complexity of DA.

Because the DA boundary has a complicated fractal structure, it cannot generally be reliably estimated analytically. Analytical methods work best when the DA boundary is dominated by a single strong resonance. In this case, single-resonance normal forms can be used [14], or a more general map-based computation can be employed [15]. Apart from DA size, typically represented by its equivalent radius, its shape and internal structure are also of interest, especially for studies of the long-term behaviour, when the required number of one-turn map iterations becomes computationally infeasible, and in the context of probing the robustness of accelerator lattice to magnetic field errors. While in 2D phase space the DA boundary is determined by homoclinic or heteroclinic tangles composed of stable and unstable manifolds of hyperbolic fixed points [16–19], in higher dimensions there is no natural boundary enclosing the orbits, and transport from small amplitudes is possible due to Arnold diffusion [20]. The internal DA structure provides information about dominant resonances and is commonly explored using chaos indicators (see, e.g. [21] and references therein), while symmetry lines also allow exploration of the DA shape [22].

In this contribution, we present a new approach to DA estimation based on a bounding set of unstable initial conditions [23]. The method provides a robust estimate of the central stable region by enclosing it with a shell of unstable points. It can be used both to characterise the DA through an equivalent radius and to explore the detailed structure of the stable domain, since full unstable orbits are used in the construction of the bounding set. We present the steps required to construct the bounding set, and we study its computational complexity and the scaling laws of the enclosed stable region [24–28]. The constructed domain is not in one-to-one correspondence with that obtained using standard ray-based DA computation, and it should be understood as a related but *distinct object*, representing the region enclosed by a cloud of unstable initial conditions.

* ivan.morozov@elettra.eu
† I.M. acknowledges support from the Elettra 2.0 project.
‡ massimo.giovannozzi@cern.ch

DIRECT DA COMPUTATION

We study the following 4D symplectic non-linear map:

$$
\begin{aligned}
q_x' &= q_x \cos\mu_x + \left(p_x + q_x^2 - q_y^2 + q_x^3 - 3q_xq_y^2\right)\sin\mu_x,\\
q_y' &= q_y \cos\mu_y + \left(p_y - 2q_xq_y - 3q_x^2q_y + q_y^3\right)\sin\mu_y,\\
p_x' &= \left(p_x + q_x^2 - q_y^2 + q_x^3 - 3q_xq_y^2\right)\cos\mu_x - q_x\sin\mu_x,\\
p_y' &= \left(p_y - 2q_xq_y - 3q_x^2q_y + q_y^3\right)\cos\mu_y - q_y\sin\mu_y,
\end{aligned}
$$

where (q_x, q_y, p_x, p_y) are the transverse normalised phase-space coordinates, $(\mu_x, \mu_y) = (2\pi\nu_x, 2\pi\nu_y)$, with ν_x, ν_y being the fractional part of the betatron tunes, and the prime indicates the coordinates after one iteration. This map is a generalisation of the 2D Hénon map [29] and despite its simplicity, it exhibits the main non-linear features of interest: a finite stability domain, resonances, and chaotic behaviour. Furthermore, it represents the transverse dynamics in a FODO cell with a sextupole and an octupole in the single-kick approximation [30].

The entire stable domain can be probed using the following polar parametrisation of rays:

$$
\begin{aligned}
(q_x,\, p_x) &= R\cos\psi\,(\cos\phi_x,\, \sin\phi_x),\\
(q_y, p_y) &= R\sin\psi\,(\cos\phi_y,\, \sin\phi_y),
\end{aligned}
$$

where $R > 0$ is the length of the rays, $\phi_x, \phi_y \in [0, 2\pi)$ are the phase angles in the canonical planes, and $\psi \in [0, \pi/2]$ controls the mixing between them. This parametrisation covers a sphere-like domain whose volume is

$$
V = \frac{1}{8}\int_0^{2\pi}\int_0^{2\pi}\int_0^{\pi/2} r^4(\psi,\, \phi_x,\, \phi_y)\,\sin(2\psi)\mathrm{d}\psi\,\mathrm{d}\phi_x\mathrm{d}\phi_y,
$$

where $r(\psi,\, \phi_x,\, \phi_y)$ is the last stable radius in a given direction and the equivalent DA radius is $\hat{r} = \left(2/\pi^2 V\right)^{1/4}$. Numerically, the volume integral is estimated by discretising the angular variables. The notation $(k,\, \ell)$ denotes k steps for ψ and ℓ steps for each of $\phi_{x,y}$, for a total of $k\times\ell^2$ rays. Along each ray, R increases in steps of ΔR until the unboundedness of the orbit is detected. Note that an alternative ray-based computation can be formulated using Monte Carlo sampling of random directions. In this case, the equivalent radius is estimated through the Hölder mean $\hat{r}^4 = 1/N\sum_i r_i^4$, where 4 is the phase-space dimension. This approach also provides a statistical uncertainty of $\hat{r}$.

An example of a direct $\hat{r}$ computation over $n = 4096$ map iterations, typical for electron machines, and $\Delta R = 0.02$ radial step size for different numbers of initial rays, is shown in Fig. 1 (top), together with the corresponding computational cost (bottom). The number of rays considered is $(k,\, \ell) = (2^i,\, 2^i)$, $2 \le i \le 6$, giving a total of 2^{3i} values. For direct computation, the equivalent radii are computed from the last stable and first unstable ray radii (black and grey crosses). Further refinement is performed by bisection (red markers), which is not part of the direct method but is included for illustration. As expected, convergence of $\hat{r}$ is observed: for $i = 4$, $\hat{r}$ differs only by 0.2% from the $i = 6$ result, while being several orders of magnitude faster to evaluate. The number of one-turn map evaluations grows approximately linearly with the number of rays and is dominated by stable initial conditions, about 99% for $(\nu_x, \nu_y) = (0.28, 0.31)$. For hadron rings, the DA boundary is defined by initial conditions with much larger escape times, corresponding to a different dynamical regime that lacks any damping. Hence, a larger number of iterations should be used for DA computation.

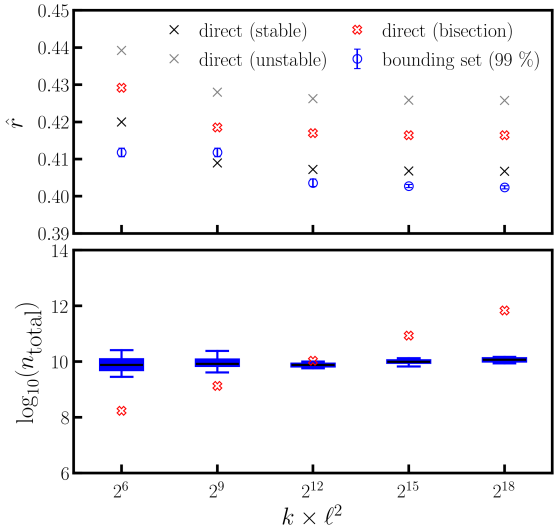

Figure 1: Equivalent DA radius (top) and corresponding computational complexity (bottom) for direct and bounding-set methods vs. the number of used rays.

THE BOUNDING-SET METHOD

The construction of the unstable bounding set that encloses the stable region is based on the following steps:

- **Domain specification**: Discretize the region of interest, specified by lower and upper bounds, using cells of side ΔS and a radial step $\Delta R = 2\Delta S$.
- **Ray-boundary specification**: Select a set of rays probing the entire domain. A ray is activated if it intersects at least one marked cell, i.e., a cell containing an unstable initial condition. For each activated ray, the first intersected marked cell is used to define the boundary.
- **Initial set construction**: The initial bounding set is constructed by moving along a small number of random rays until an unbounded orbit is found. The entire unstable orbit is then used to mark as unstable the cells containing its points.
- **Ray-based boundary filtering**: For each activated ray, retain only the first intersected marked cell. All other marked cells are discarded at this stage, although a copy of the full marked-cell set can be saved and updated.
- **Domain expansion**: Generate new initial conditions from the ray-based filtered cells using either uniform or angle-based random sampling.
- **Repeat expansion & filtering steps**: Repeat steps until all rays are activated or a prescribed number of activated rays is reached.

- **Equivalent radius computation**: Use the resulting boundary cells to compute the ray-based equivalent DA radius, or use the Hölder mean if the threshold-based termination is used.

The results obtained using the above steps and the parameters used in the direct calculation are shown in Fig. 1. For the bounding-set method, the rays are used to explore the boundary of the DA. Similarly to the direct computation, the final value converges as the number of rays is increased. The estimated radius is systematically smaller than that obtained from the direct computation. The main reason is that the atomic objects of the bounding-set method are hypercubes, that is, full-dimensional, finite-size objects, whereas the rays used in the direct method can probe regions smaller than the cell size. The finite cell size seems to provide a more robust mean of DA estimation, since it excludes narrow regions that are of limited practical interest. The computational cost depends weakly on the number of rays used to define the boundary and, for the largest ray set, is about two orders of magnitude lower than that of the direct computation. The error bars, obtained from several initial-set samples, demonstrate the small spread achieved with a large number of rays.

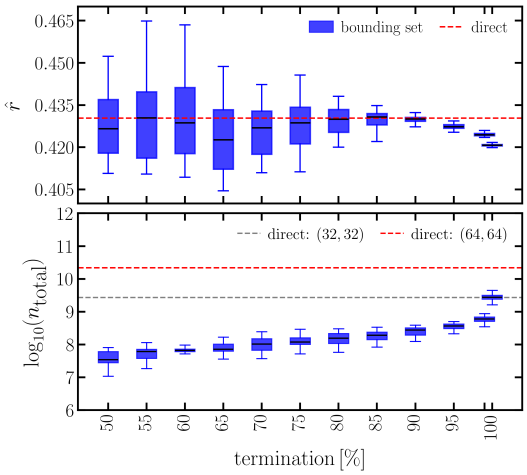

Figure 2: Equivalent DA radius (top) and computational complexity (bottom) for different termination thresholds.

A comparison of the distribution of explored ray radii demonstrates that direct and bounding-set methods explore similar phase-space regions even in the presence of termination. Complete boundary convergence is achieved, on average, in 70 rounds of domain expansion and filtering over 32 realisations using $(64, 64)$ rays. Figure 2 illustrates how termination, defined by archiving a prescribed percentage of activated rays, affects the equivalent radius and computational complexity.

Figure 3 shows the fitted equivalent DA radius scaling-law curves $\hat{r}(n) = \rho(\kappa/2\mathrm{e})^{\kappa}/\ln^{\kappa}(n)$ [28] obtained using the data points indicated by the grey lines. The average results over 32 different realisations, including statistical uncertainties, are fitted for the bounding-set method. The shaded area represents the 95% confidence interval, and the prediction of last point is accurate to better than 1%.

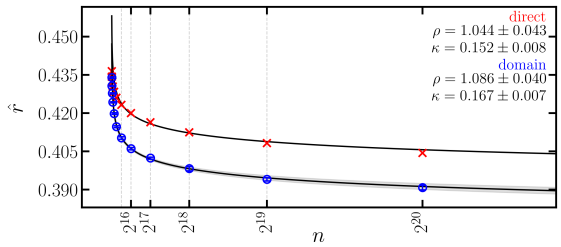

Figure 3: Fit of the DA scaling law for the direct (red) and bounding-set (blue) methods using data indicated by the vertical lines.

The generated ray boundary can be used further to grow the domain, with new marked cells being added without ray-based filtering. This allows detailed exploration of the shape of the stable domain, and visualisation of its projections (see Fig. 4 and [31] for interactive 3D projections). The full 4D bounding set is constructed, and its projections are compared with boundaries obtained from 2D ray tracking. The projected boundary closely matches the ray-based one, except in the horizontal plane, where the project of the bounding set may represent a singular behaviour of the dynamics.

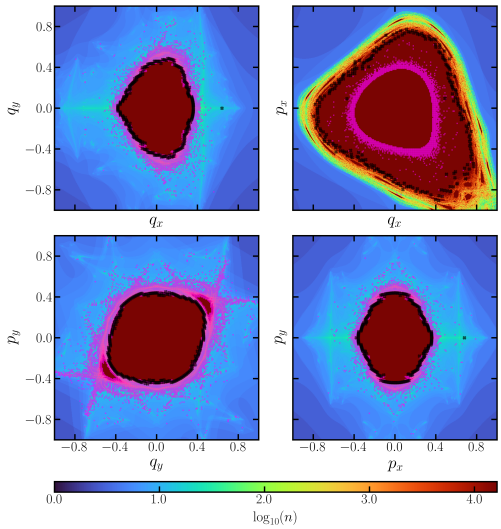

Figure 4: Projections of the bounding set (magenta) and comparison with 2D ray-based DA computation (black) and grid survival scans for the four possible 2D projections.

CONCLUSIONS AND OUTLOOK

A new method for DA estimation and characterisation is presented, based on a bounding set of unstable initial conditions. By using information from entire unstable orbits, rather than only from their initial conditions, the method provides a conservative estimate of the DA region and its geometric shape. For a large number of rays, it is also more computationally efficient than direct ray-based DA computation. Initial studies with the Hénon map demonstrate that the DA scaling law is respected by the bounding set. Further studies with a larger number of iterations are foreseen to assess the method's behaviour for applications to hadron accelerators.

REFERENCES

[1] L. Evans and P. Bryant, "LHC Machine", *J. Instrum.*, vol. 3, no. 08, p. S08001, 2008. doi:10.1088/1748-0221/3/08/S08001

[2] A. Abada *et al.*, "FCC-hh: The Hadron Collider", *Eur. Phys. J. Spec. Top.*, vol. 228, no. 4, pp. 755–1107, 2019. doi:10.1140/epjst/e2019-900087-0

[3] M. Benedikt *et al.*, "Future circular collider feasibility study report", *Eur. Phys. J. Spec. Top.*, vol. 234, no. 19, pp. 5713–6197, 2025. doi:10.1140/epjs/s11734-025-01967-4

[4] W. Scandale, "Dynamic aperture", CERN, Geneva, Switzerland, CERN-SL-94-24-AP, 1995. doi:10.5170/CERN-1995-006.109

[5] K. Oide *et al.*, "Design of beam optics for the future circular collider e^+e^- collider rings", *Phys. Rev. Accel. Beams*, vol. 19, no. 11, p. 111005, 2016. doi:10.1103/PhysRevAccelBeams.19.111005

[6] E. H. Maclean, R. Tomás, F. Schmidt, and T. H. B. Persson, "Measurement of nonlinear observables in the Large Hadron Collider using kicked beams", *Phys. Rev. ST Accel. Beams*, vol. 17, no. 8, p. 081002, 2014. doi:10.1103/PhysRevSTAB.17.081002

[7] E. Todesco and M. Giovannozzi, "Dynamic aperture estimates and phase-space distortions in nonlinear betatron motion", *Phys. Rev. E*, vol. 53, no. 4, pp. 4067–4076, 1996. doi:10.1103/PhysRevE.53.4067

[8] B. Riemann, M. Aiba, J. Kallestrup, and A. Streun, "Efficient algorithms for dynamic aperture and momentum acceptance calculation in synchrotron light sources", *Phys. Rev. Accel. Beams*, vol. 27, no. 9, p. 094002, 2024. doi:10.1103/PhysRevAccelBeams.27.094002

[9] M. Giovannozzi, E. Maclean, C. E. Montanari, G. Valentino, and F. F. Van der Veken, "Machine Learning Applied to the Analysis of Nonlinear Beam Dynamics Simulations for the CERN Large Hadron Collider and Its Luminosity Upgrade", *Information*, vol. 12, no. 2, 2021. doi:10.3390/info12020053

[10] J. Wan and Y. Jiao, "Machine learning enabled fast evaluation of dynamic aperture for storage ring accelerators", *New J. Phys.*, vol. 24, no. 6, p. 063030, 2022. doi:10.1088/1367-2630/ac77ac

[11] M. Casanova, B. Dalena, L. Bonaventura, and M. Giovannozzi, "Ensemble reservoir computing for dynamical systems: prediction of phase-space stable region for hadron storage rings", *Eur. Phys. J. Plus*, vol. 138, no. 6, p. 559, 2023. doi:10.1140/epjp/s13360-023-04167-y

[12] D. Di Croce, M. Giovannozzi, C. E. Montanari, T. Pieloni, S. Redaelli, and F. F. Van der Veken, "Assessing the performance of deep learning predictions for dynamic aperture of a hadron circular particle accelerator", *Instruments*, vol. 8, no. 4, 2024. doi:10.3390/instruments8040050

[13] C. E. Montanari *et al.*, "Machine learning techniques for uncertainty estimation in dynamic aperture prediction", *Computers*, vol. 14, no. 7, 2025. doi:10.3390/computers14070287

[14] A. Bazzani, M. Giovannozzi, G. Servizi, E. Todesco, and G. Turchetti, "Resonant normal forms, interpolating hamiltonians and stability analysis of area preserving maps", *Physica D*, vol. 64, no. 1, pp. 66–97, 1993. doi:10.1016/0167-2789(93)90249-Z

[15] T. Zolkin, S. Nagaitsev, I. Morozov, and S. Kladov, "Geometry of almost-conserved quantities in symplectic maps", *Chaos, Solitons Fractals*, vol. 208, p. 118059, 2026. doi:10.1016/j.chaos.2026.118059

[16] M. Giovannozzi, "Analysis of the stability domain for the hénon map", *Phys. Lett. A*, vol. 182, no. 2, pp. 255–260, 1993. doi:10.1016/0375-9601(93)91067-F

[17] M. N. Vrahatis, T. C. Bountis, and M. Kollmann, "Periodic orbits and invariant surfaces of 4-D nonlinear mappings", *Int. J. Bifurcation Chaos*, vol. 06, no. 08, pp. 1425–1437, 1996. doi:10.1142/S0218127496000849

[18] M. Giovannozzi, "Stability domain of planar symplectic maps using invariant manifolds", *Phys. Rev. E*, vol. 53, no. 6, pp. 6403–6412, 1996. doi:10.1103/PhysRevE.53.6403

[19] S. Anastassiou, T. Bountis, and A. Bäcker, "Homoclinic points of 2D and 4D maps via the parametrization method", *Nonlinearity*, vol. 30, no. 10, p. 3799, 2017. doi:10.1088/1361-6544/aa7e9b

[20] V. I. Arnold, "Instability of dynamical systems with several degrees of freedom", in *Collected Works: Representations of Functions, Celestial Mechanics and KAM Theory, 1957–1965*, A. B. Givental *et al.*, Eds. Berlin, Heidelberg: Springer Berlin Heidelberg, 2009, pp. 423–427. doi:10.1007/978-3-642-01742-1_26

[21] A. Bazzani, M. Giovannozzi, C. E. Montanari, and G. Turchetti, "Performance analysis of indicators of chaos for nonlinear dynamical systems", *Phys. Rev. E*, vol. 107, no. 6, p. 064209, 2023. doi:10.1103/PhysRevE.107.064209

[22] T. Zolkin, S. Nagaitsev, I. Morozov, S. Kladov, and Y.-K. Kim, "Isochronous and period-doubling diagrams for symplectic maps of the plane", *Chaos, Solitons Fractals*, vol. 198, p. 116513, 2025. doi:10.1016/j.chaos.2025.116513

[23] I. Morozov, "domain", *GitHub repository*, 2026. https://github.com/i-a-morozov/domain

[24] N. N. Nekhoroshev, "An Exponential Estimate of the Time of Stability of Nearly-Integrable Hamiltonian Systems", *Russ. Math. Surv.*, vol. 32, no. 6, p. 1, 1977. doi:10.1070/RM1977v032n06ABEH003859

[25] A. Bazzani, S. Marmi, and G. Turchetti, "Nekhoroshev estimate for isochronous non resonant symplectic maps", *Celestial Mech. Dyn. Astron.*, vol. 47, no. 4, pp. 333–359, 1989. doi:10.1007/BF00051010

[26] G. Turchetti, "Nekhoroshev stability estimates for symplectic maps and physical applications", in *Number Theory and Physics*, pp. 223–234, 1990.

[27] M. Giovannozzi, W. Scandale, and E. Todesco, "Dynamic aperture extrapolation in the presence of tune modulation", *Phys. Rev. E*, vol. 57, no. 3, pp. 3432–3443, 1998. doi:10.1103/PhysRevE.57.3432

[28] A. Bazzani, M. Giovannozzi, E. H. Maclean, C. E. Montanari, F. F. Van der Veken, and W. Van Goethem, "Advances on the modeling of the time evolution of dynamic aperture of hadron circular accelerators", *Phys. Rev. Accel. Beams*, vol. 22, no. 10, p. 104003, 2019. doi:10.1103/PhysRevAccelBeams.22.104003

[29] M. Hénon, "Numerical study of quadratic area-preserving mappings", *Q. Appl. Math.*, vol. 27, p. 291, 1969. doi:10.1090/qam/253513

[30] A. Bazzani, G. Servizi, E. Todesco, and G. Turchetti, *A normal form approach to the theory of nonlinear betatronic motion*. Geneva: CERN, 1994. doi:10.5170/CERN-1994-002

[31] I. Morozov, 4D Hénon mapping bounding set 3D projections, 2026, https://henon4d.streamlit.app/.